Structural Investigations on ZnO Doped with Al$_2$O$_3$

Gomaa-El Damrawi[*], Naer Baker, Ahamed Al-kalbani

Physics Department, Faculty of Science, Mansoura University, Mansoura, Egypt

Abstract

The phase change and micro-structure determination of both ZnO and ZnO-Al$_2$O$_3$ matrices have been investigated using nuclear magnetic resonance spectroscopy (NMR), X-ray diffraction (XRD), energy-dispersive X-ray spectroscopy (EDS) and transition electron microscopy (TEM) with selected area electron diffraction (SAED). The effect of both material structure and thermal heat treatment (THT) at different temperatures on the crystallization nature of ZnO and Al$_2$O$_3$-ZnO nanoparticles was recorded. A well-controlled crystallization extraction was followed by crystalline phase formation. The matrix structure of ZnO-Al$_2$O$_3$ is completely changed by partially replacing ZnO with Al$_2$O$_3$. It is confirmed that the quantity and type of crystalline ZnO phases are affected by changing glass structure and heat treatment temperature. The crystalline structure in the ZnO matrix is fully transformed into an amorphous one by introducing Al$_2$O$_3$ to ZnO. This finding was due to the development of the material structure through non-bridging bonds (NBB). The NBB formation can reduce the unified and symmetrical structure leading to the formation of the less orderly network. On the other hand, the amorphous phases are converted into the crystalline (ZnAl$_2$O$_4$) one, especially in heat-treated ZnO-Al$_2$O$_3$ glasses. This is because the THT mechanism will allow the process of phase separation that leads to crystallization to take place. The structure and size of various crystals can be identified by TEM microscopy. The ^{27}AlNMR analysis showed a considerable change in chemical shift upon increasing Al$_2$O$_3$. Sample containing 1 w% Al$_2$O$_3$ contains defective AlO$_4$ units. While sample containing 5 w% Al$_2$O$_3$ has a more shielded structure due to formation of strengthened Al$_4$-O-Zn$_4$ bonds

1. Introduction

Incorporation of aluminium oxide as a doping in ZnO network assists to analyze different structural and physical properties of the base matrix. Previous studies were conducted on aluminum-doped ZnO nanocrystalline aggregates prepared using a method of colloid chemistry [1]. The morphological and some structure effects of aluminium doping concentrations have been reported. The results indicated that, the doping of Al ions changes the structure of ZnO crystal and reduces the crystalline grain size. ZnO doped with tellurium Te has been also prepared and studied by different techniques [2]. The related results revealed that ZnO doped with Te had higher photocatalytic performance than undoped ZnO. The results of the X-ray diffraction of the indium doped ZnO [3] showed that the product obtained is characterized by a crystalline hexagonal structure with a preferred orientation towards (002) plane. TEM microscopy revealed that the particle size is increased with an increase in the doping concentration. The morphology varied from particles to aggregated spheres. Chen et al [4] used the sol-gel process to prepare ZnO doped with Al atoms (0-9%). The influence of thermal heat treatment on the properties and

* Corresponding author

E-mail address: gomaaeldamrawi@gmail.com (Gomaa-El D.)

structure of the samples prepared had also been studied. They found no variation in XRD spectra of ZnO and ZnO doped batches. This may indicate that Zn atoms can simply be replaced by the micro Al ions without any change in the range structure ordered. In addition, the effect on surface structure of thermal annealing and heat treatment temperature was also observed. It has been concluded that the grain size decreases as the temperature increases. The degree of crystallinity is affected by the changing temperature of annealing. The concentration of crystalline species is increased, which plays a role in reducing the residual stress which in turn enhances the physical properties of the studied material.

Most of the previous studies concentrated on the zinc doped with atomic elements like Te, Al, and In. To our knowledge, doping of ZnO nanoparticles with Al_2O_3 is limited. No magnetic resonance research on these materials has been done. Our goal is to examine the structural role of Al_2O_3 across the ZnO matrix during this study. Specific spectroscopic techniques will be performed to get specific analysis which have to carry out on the pure ZnO and Al_2O_3 doped ZnO.

2. Experimental

2.1. Sample Preparation

Pure ZnO is prepared by the sol-gel method. A calculated amount of Zn acetate is added to the reaction mixture which has been stirred for 2 hours. Then the appropriate amount of ammonia solution (30%) is added drop by drop to the solution until formation of a white precipitate. The acetate groups convert zinc acetate into zinc oxide which is organized from the product solution during the process of precipitation. The obtained precipitate was washed several times with ethanol and water then dried at 80°C for 12 hours. The resultant powered sample was calcined at different temperature 400, 500, and 600°C to evaporate carbonate, nitrate and water.

To prepare Al_2O_3-ZnO material, aluminium nitrate nonahydrate $(Al(NO_3)_{3.9}H_2O)$ was added into the solution to serve as the aluminium source. The calculated amount $(Al(NO_3)_{3.9}H_2O)$ was added to reaction mixture followed by precipitation step. The final powdered samples were calcined at different temperatures.

2.2. Measurements

X-Ray diffraction measurements are carried out with Shimadzu X-ray diffract meter (Dx-30, Metallurgy institute, El Tebbin-Cairo). The peak position and intensity values used to identify the type of material were compared with patterns in the international powder diffraction file (PDF) database complied by joint commite for powder diffraction standards (JCPDS)

NMR measurements were carried out at ambient temperature on a JEOL RESONANCE GSX-500 spectrometer operating at a high external magnetic field (11.747 T). ^{27}Al NMR spectra were measured at the resonance frequency of 130.2 MHz, using a 3.2 mm MAS NMR probe operated at a rotor frequency of 15 kHz. Typical pulse lengths were 2.5 μs and 60 seconds delay time was sufficient to enable relaxation.

TEM provides topographical, morphological and crystalline information of the distributed particles, the powdered samples were dispersed in ethanol and a drop of this solution was spread on carbon coated copper grid to view images. TEM image and particle size were obtained using (JEOL JEM-1230 operated at 120 KV, Analytical Lab, Mansoura University)

3. Results and Discussion

^{27}Al MAS-NMR spectroscopy was applied to examine both Al_2O_3 as uni-composition and the binary ZnO-Al_2O_3 structures. There are three resonances lines are identified at 10, 35 and 70 ppm on the ^{27}Al NMR spectra of pure Al_2O_3 matrix, figure 1. These three resonance lines were assigned to the AlO_6, AlO_5 and AlO_4 coordinated units respectively [5-8]. Mixing Al_2O_3 with a higher ZnO content transforms the more symmetrical AlO_5 groups into asymmetric AlO_4 which is the only units observed in the ZnO-Al_2O_3 matrix containing 1 w% Al_2O_3, see figure 2 a. There is only one resonance peak existed at approximately 60 ppm. More specifically, ^{27}Al isotropic chemical shift was obtained along the 5% Al_2O_3, see figure 2 (b). Only one resonance peak is existed at approximately 42 ppm. Change the chemical shift from 60 to 42 ppm may reflect the increasing concentration of Al-O-Zn bonds in sample of 5 w% Al_2O_3. In such a case Zn can be found in the second coordination of Al which leads to shielding AlO_4 groups.

The spectrum presented by figure 1 confirmed that Al_2O_3 acts as an intermediate oxide [5-8] comprising Al in 6- and 5-coordination with oxygen atoms, in addition to the dominant 4-coordinated species. ZnO-Al_2O_3 has ratios ZnO/Al_2O_3 >>1, therefore this mixed matrix contains only 4-coordinated aluminium [8]. The glass's average isotropic chemical shift decreases with increasing Al_2O_3 contents in ZnO-Al_2O_3 glass, which may indicate an improvement in the polymerization status of aluminium units. The chemical shifts for the ZnO-Al_2O_3 glass is systematically displaced to lower value that can be associated with a rearrangement of Zn and Al in the next neighboring coordination environment for the central Al atom.
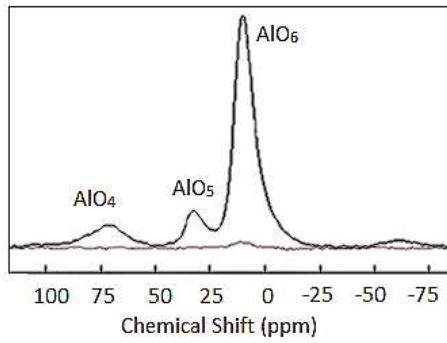
Figure 1. ^{27}Al NMR spectra for Al_2O_3 treated at 500°C. The spectra contain AlO_6, AlO_5 and AlO_4 coordination.
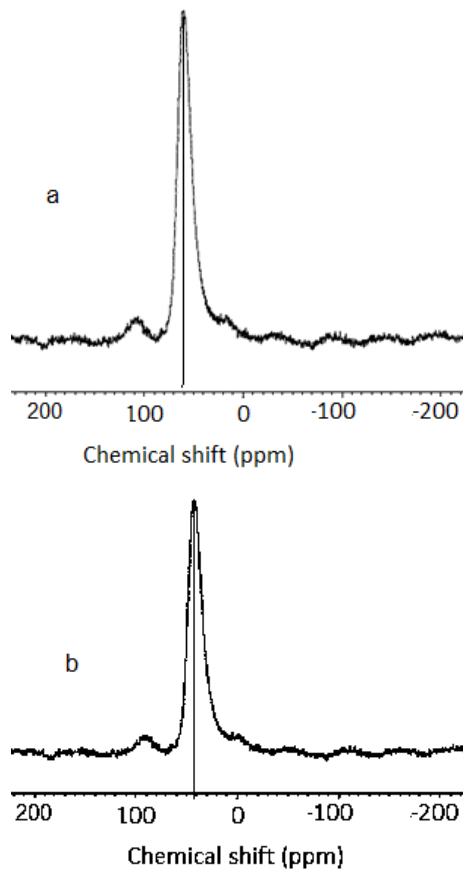

Figure 2. NMR spectra of samples containing 1 and 5 w% Al_2O_3, (a) and (b) respectively.

Based on a correlation between NMR spectra of figures 1 and 2, it can clearly be inferred that in the ZnO-Al_2O_3 samples, some of ZnO are consumed in the development of non-bridging bond (NBB) in AlO_4 units because ZnO plays an intermediate role [9-11]. The incorporated zinc oxide in glass in ZnO-Al_2O_3 matrix is expected to acts as an intermediate oxide either as network former or as network modifier. As a former, ZnO enters the network with ZnO_4 structural units and as network modifier, zinc ions are octahedrally coordinated and behaves like any other conventional alkali oxide. The role of former species resulting in the formation of Zn-O-Al bonds. This suggestion seems to be in comparison to the previous reported observation [5-8] as it has been confirmed that AlO_4 units with NBB increases when AlO_5 is transformed into AlO_4 species. The observations based on NMR spectroscopy is further confirmed from EDEX spectra of samples containing 5% Al_2O_3 and 95 ZnO, figure 3. It can simply observe that there are three peaks for Zn, one appeared at 1 KeV which represent ZnO as a modifier. The other two spectra raised at 8.5 and 9.5 KeV represent ZnO as a former and ZnO molecules coordinated with AlO_4 only, respectively.
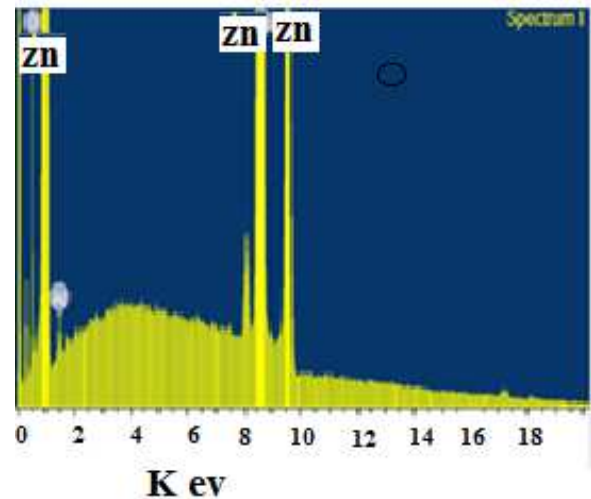

Figure 3. EDEX spectra of sample containing 5% aAl_2O_3 and 95 ZnO.

The presence of AlO_4 groups in the ZnO network has a significant effect on the investigative range-ordered structure. The consequence of the introduction of Al_2O_3 turns the crystalline ZnO material (figure 4) into amorphous phases (figure 5). Such effect is explored from XRD spectra of Figures 4 and 5.

Figure 4 shows the X-ray diffraction patterns of ZnO as prepared and heat treated at 400, 500 and 600°C. All the analyzed specimens had diffraction peaks of approximately $2\theta = 31.8°$, $34.2°$, $36.3°$, $47.4°$, $56.76°$, $62.9°$, $68.1°$ and $77.1°$. These lines were attributed to different planes of hexagonal crystalline phase of ZnO (JCPDF: 891397) [12, 13]. The positions of diffraction lines were indexed respectively to (100), (002), (101), (102), (110), (103), (200), (112) and (201) planes. It is noticed that, the position of the diffraction lines does not change even with increasing heat treatment temperature which means that the well-formed crystalline species are saturated with similar Zn-O-Zn bonds which have the same nature. Nevertheless, the intensity of the diffraction lines increases dramatically to a maximum at 600°C, resulting in the thermal temperature being able to activate the phase separation process needed to improve the crystallinity.
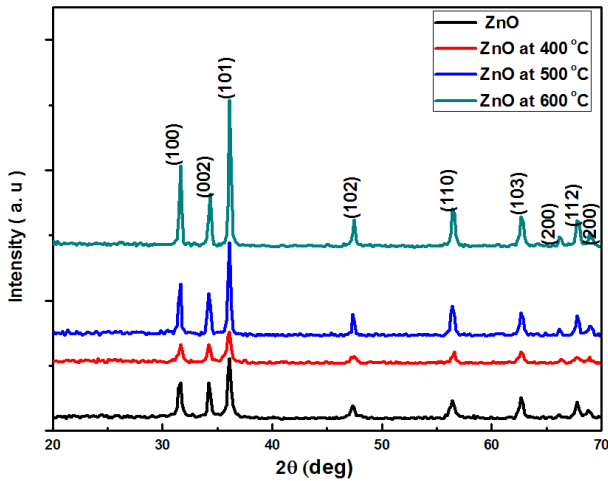
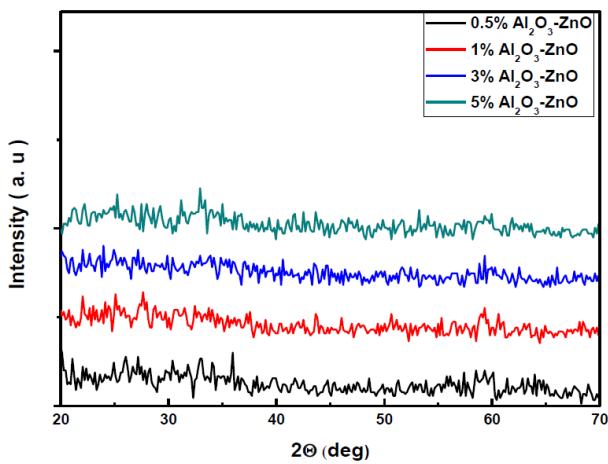**Figure 4.** XRD spectra of untreated and thermally treated ZnO.

Figure 5. XRD spectra of Al$_2$O$_3$-ZnO mixed materials.

There is a difference not only between the XRD pattern of pure ZnO and Al$_2$O$_3$-ZnO (figures 4 and 5), but also between the NMR alumina spectra and their ZnO-modified counterpart (figures 1 and 2). Due to a reduction in the AlO$_5$ groups and a concomitant rise in AlO$_4$, this difference is perceived. This suggests that the alumina and ZnO sites are changed. In the presence of Al$_2$O$_3$ in the ZnO network, these changes played the role of creating less ordered structure, figure 5. By forming Zn$_4$-O-Al$_4$ or Zn-O-Al$_5$ non-symmetric bonds, since Al$_2$O$_3$ will simply change both the bond angles and lengths of O-Zn-O normal bond.

TEM microscopy is used to examine the morphology and particle size of untreated ZnO and the thermally treated samples at 400, 500 and 600°C. Figure 6(a, b, c, d) displays the micrographs obtained with their electron diffraction patterns. The TEM micrograph of untreated ZnO, figure 6(a), shows different shapes and size of particles in the range of 20-35 nm which in a good agreement with XRD pattern, since the order structure of the investigated sample is confirmed. The micrograph of sample treated thermally at about 400°C, figure 6(b), shows spherical particles shape of lower particle size compared with that of untreated sample. The particle shapes and size are changed toward increasing values in the sequence of increasing THT from 400 to 600°C, figure 6(b, c, d). The selected area of electron diffraction (SAED) displays pattern showing diffraction rings assigned to the ZnO nanoparticles in the form of polycrystalline structure, which have been confirmed by XRD spectra of the investigated samples.
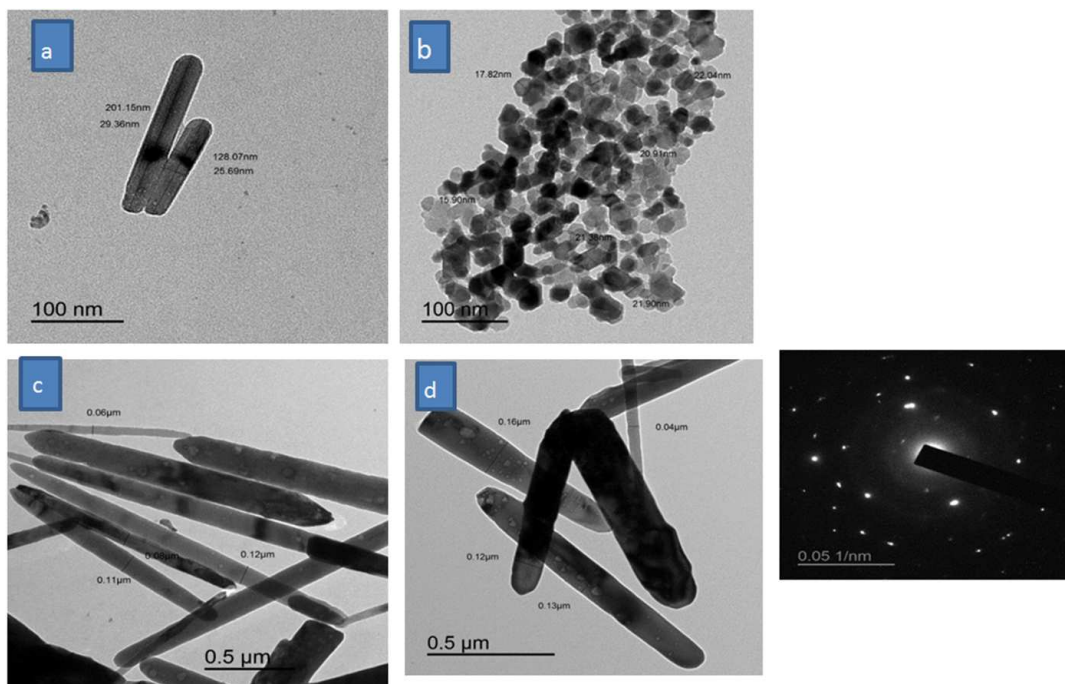

Figure 6. TEM Micrograph of pure ZnO (a) as obtained (b) treated at 400°C (c) at 500°C and (d) at 600°C.

Figure 7 shows the X-ray diffraction patterns of Al_2O_3-ZnO samples as prepared and heat treated at 400, 500 and 600°C. The untreated composition showed an amorphous structure but all thermally treated samples had sharp diffraction peaks. These lines were attributed to different planes of hexagonal crystalline phase containing Zn and Al. It is noticed that, the positions of the diffraction lines do not change even with increasing heat treatment temperature which means that the well-formed crystalline species are saturated with similar Zn-O-Al bonds which have the same nature. Nevertheless, the intensity of the diffraction lines increases dramatically to a maximum at 600°C, resulting in the thermal temperature being able to activate the phase separation process needed to improve the crystallinity [14-16]. It can be noticed from figure 6 that no peaks in XRD pattern of untreated sample, but with increasing the tempering temperature more intense peak are found to become maximum at 600°C. Increasing crystallinity may attributed to the high dispersion of Al_2O_3 on the surface of ZnO [16].

Figure 8 (a, b, c and d) represents TEM micrographs of untreated Al_2O_3-ZnO and the thermally treated samples at 400, 500 and 600°C. The micrograph of untreated sample, figure 8(a),

shows the different shapes and size of bar like shapes. The micrograph of sample treated thermally at about 400°C, 500°C and 600°C figure 8 (b, c, d), shows spherical particles shape beside few of the rod like shapes. The particles are accumulated to form condensed aggregations of an increasing density. This leads that, increasing the temperature of thermal treating glasses will improve the separation of crystalline species from the main matrix and accumulated as a crystalline matrix.
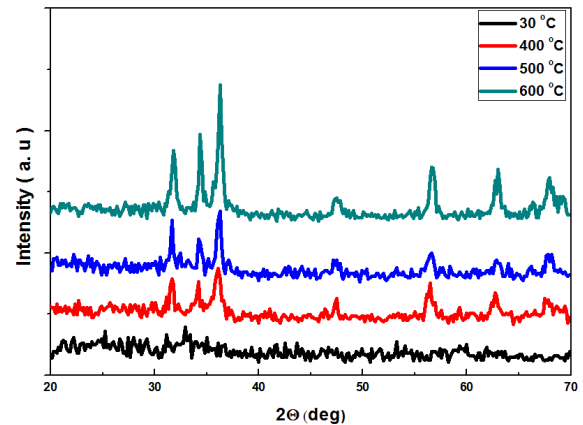

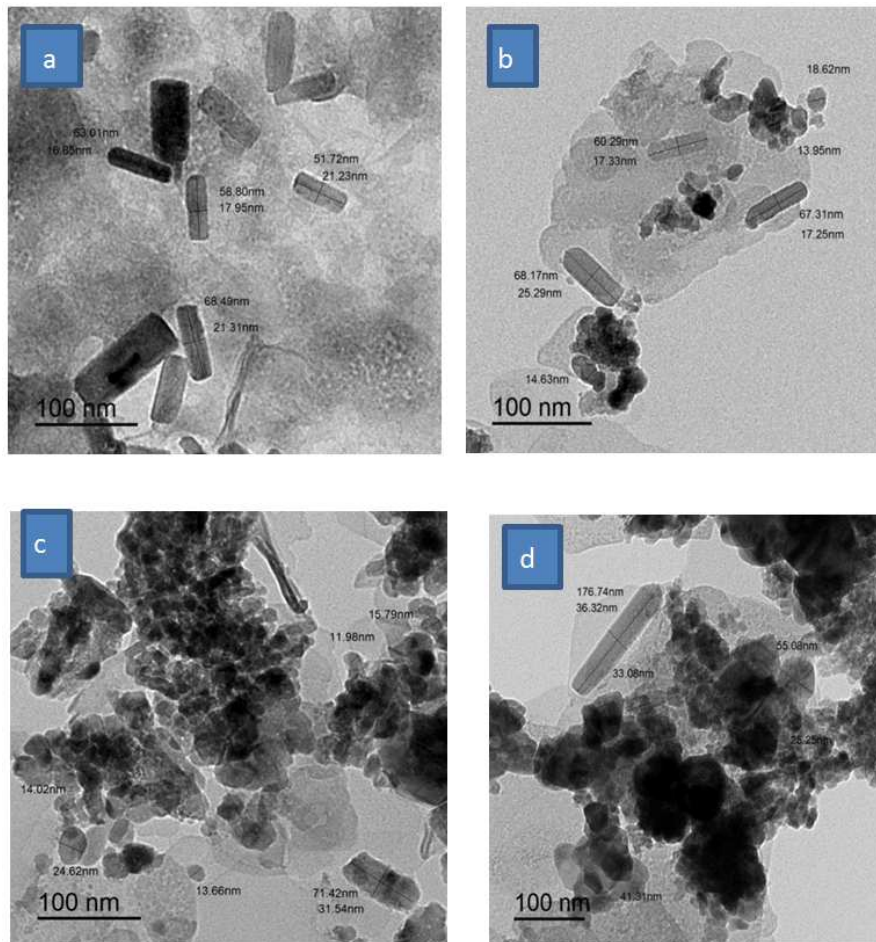**Figure 7.** XRD of 5% Al_2O_3/ZnO calcinated at different temperatur.

Figure 8. TEM Micrograph of pure ZnO-Al_2O_3 samples containing 5 mol% Al_2O_3 (a) as obtained (b) treated at 400°C (c) at 500° and (d) at 600°C.

4. Conclusion

The ^{27}Al NMR analysis showed a considerable change in chemical shift upon increasing Al_2O_3. Sample containing 1 w% Al_2O_3 contains defective AlO_4 units. While sample containing 5 w% Al_2O_3 has a more shielded structure due to formation of strengthened Al_4-O-Zn_4 bonds. The effect of both material structure and thermal heat treatment (THT) at different temperatures on the crystallization nature of ZnO and Al_2O_3-ZnO glasses has been studied by XRD and TEM. The quantity and type of crystalline ZnO are affected by changing glass structure and heat treatment temperature. The crystalline structure in the ZnO matrix is fully transformed into an amorphous one by introducing Al_2O_3 to ZnO. This finding was approved by NMR results, since the main structure of ZnO was developed through formation of non-bridging bonds (NBB). The NBB formation can reduce the unified and symmetrical structure leading to the formation of the less orderly network. The dominant amorphous structure of ZnO-Al_2O_3 network is converted into the crystalline ($ZnAl_2O_4$) one, especially in heat-treated ZnO Al_2O_3 glasses. THT allows the process of phase separation to carry out which leads to more crystallization.

References

[1] J. Zhang, W. Que, Y. Yuan, P., Zhong., andY. Liao. Preparation of Al-doped ZnO nanocrystalline aggregates with enhanced performance for dyeadsorption, Science China Physics. Mechanical and Astromomy 55 (7) (2012) 1198-1202

[2] N. Shanmugam, S. Suthakaran, N. Kannadasan, and K. Sathishkumar, Synthesis and characterization of Te doped ZnO nanosheets for photocatalyric applications. JO Heterocyclics 105 (2015) 15-20

[3] K. S. Khashan, and M. Mhdi, Preparation of Indium-Doped zinc oxide nanoparticles by pulsed laser ablation in liquid technique and therir characterization. Applied Nanoscience 7 (8) (2017) 589-596.

[4] K. J Chen. T. H Fang, F. Y. Hung, L. W. Ji, S. J Chang. S. J Young,, and Y. I Hsiao, The crystallization and physical properties of Al-doped ZnO nanoparticles. Applied surface Science, 254 (18) (2008) 5791-5795.

[5] Y. Fujimoto, M. Nakatsuka, ^{27}Al NMR structural study on aluminum coordination state in bismuth doped silica glass, Journal of Non-Crystalline Solids 352 (2006) 2254–2258

[6] S. H. Risbud, R. J. Kirkpatrick, A. P. Taglialavore, B. Montez, J. Am. Ceram. Soc. 70 (1987) 10

[7] M. Schmiicker, K. J. D. MacKenzie, H. Schneider, R. Meinhold, J. Non-Cryst. Solids 217 (1997) 99.

[8] G. El-Damrawi, A. K. Hassan, A. Shahboub, ^{31}P and ^{27}Al nuclear magnetic resonance studies on silver phosphate glasses, Magn. Reson. Solids 20 (2018), 18202.

[9] L. Balua, R. Amaravel, and R. Ezhil Pavaib, Effect of Zno on Physical, Structural and Mechanical Properties of B_2O_3-Na_2O-ZnO glasses, IOSR Journal of Applied Physics (IOSR-JAP) e-ISSN: 2278-4861. Volume 8, Issue 6. -Dec. (2016) 140-146

[10] H. S. Liu and T. S. Chin, "The new zinc barium metaphosphate glasses. (50-x) BaO-xZnO-50P_2O_5" Physics and Chemistry of Glasses, 38 (1997) 123–131.

[11] K. A. Matori, M. H. M. Zaid, H. A. A. Sidek, M. K. Halimah, Z. A. Wahab, and M. G. M. Sabri, "Influence of ZnO on the ultrasonic velocity and elastic moduli of soda lime silicate glasses," International Journal of Physical Sciences, 5 (2010) 2212–2216

[12] M. Malini, M. Thirumavalavan, W. Y. Yang, J. F. Lee, G. Annadurai, A versatile chitosan/ZnO nanocomposite with enhanced antimicrobial properties, Int. J. Biol. Macromol. 80 (2015) 121–129.

[13] M. Karpuraranjith, S. Thambidurai, Chitosan/zinc oxide-polyvinylpyrrolidone (CS/ZnO- PVP) nanocomposite for better thermal and antibacterial activity, Int. J. Biol. Macromol. 104 (2017) 1753–1761.

[14] JA Johnson, JKR Weber, AI Kolesnikov, and S Schweizer, Crystallization in heat- treated fluorochlorozirconate glasses, J Phys Condens Matter. 16; 21 (37) (2009) 3751031–3751036.

[15] S. Dalal, S. Khasa, M. S. Dahiya, ArtiYadav, A. Agarwal, S. Dahiya, Journal of Asian Ceramic Societies 3 (2015) 234-239.

[16] M. -K. Song, M-Y. Lee, J-H. Seo, M, H. Kim, and S. Y. Yang, Journal of Nanomaterials Volume Article ID 151532 (2015) 6.